

Interaction and Conformation of Aqueous Poly(*N*-isopropylacrylamide) (PNIPAM) Star Polymers below the LCST

Xiaolong Lang,[†] William R. Lenart,[†] Jessie E. P. Sun,[‡] Boualem Hammouda,[§] and Michael J. A. Hore^{*,†,§}

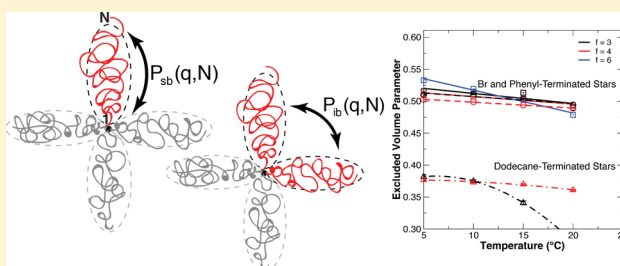
[†]Department of Macromolecular Science and Engineering, Case Western Reserve University, 10900 Euclid Avenue, Cleveland, Ohio 44106, United States

[‡]Laurel School, One Lyman Circle, Shaker Heights, Ohio 44122, United States

[§]NIST Center for Neutron Research, 100 Bureau Drive, Gaithersburg, Maryland 20899, United States

Supporting Information

ABSTRACT: Small-angle neutron scattering (SANS) is used to measure the conformation and solution thermodynamics of low dispersity, star branched poly(*N*-isopropylacrylamide) (PNIPAM) in water using a newly developed form factor for star-branched polymers with excluded volume, in conjunction with the random phase approximation (RPA). Star PNIPAM is synthesized using both ATRP and RAFT, allowing the terminal group and number of arms to be precisely tuned from $f = 3$ to 6 arms, with bromine, phenyl, and dodecane terminal moieties. SANS measurements show that both the number of arms (f) and synthetic route (i.e., ATRP or RAFT) play a dominant role in the solution behavior of PNIPAM in relation to the interaction parameters, conformation of the arms of the polymer, and clustering/association of the polymers below the LCST. Dodecane-terminated PNIPAM polymers form small, sub-20 nm globules in solution, whereas phenyl- and bromine-terminated polymers form large, micrometer-scale clusters of nearly-Gaussian polymer chains. Multiangle light scattering (MALS) is used to probe the large clusters, finding that their size increases slightly with temperature but is largely independent of terminal group chemistry.



1. INTRODUCTION

A polymer differs from a small molecule in several ways, one of which is how its conformation changes with respect to solvent quality. The conformation of a polymer is represented by the manner in which the radius of gyration (R_g) scales with the degree of polymerization (N). In general, $R_g \sim N^\nu$, where ν is an excluded volume parameter that reflects the quality of the solvent and, in turn, the excluded volume (ν_e) of the polymer chain due to two-body interactions between monomers. In a poor solvent, interactions between chemically similar monomers are more favorable than those between the monomers and the solvent, leading to a globular structure with $\nu \approx 1/3$ and $\nu_e < 0$. As the interactions between the solvent and monomers become more favorable, meaning interactions between pairs of monomers become increasingly repulsive, both the excluded volume parameter and excluded volume increase, giving $\nu = 1/2$ and $\nu_e = 0$ at the theta condition and $\nu \approx 3/5$ and $\nu_e > 0$ in a good solvent.¹

When confined, polymer chains with excluded volume are typically elongated as compared to their equilibrium, non-confined state. This effect has been observed for cylindrically confined polymers,² planar polymer brushes,^{3–5} and polymers that are confined by virtue of being grafted to the surface of a nanoparticle.^{6–9} In the latter example, near the surface of a spherical nanoparticle, polymer chains at high grafting density adopt a size that scales as $R \sim N^{0.8}$ in the concentrated polymer brush region (CPB) and later transition to a more ideal

conformation beyond a cutoff distance (r_c) from the nanoparticle surface in the semidilute polymer brush region (SDPB)—as observed by dynamic light scattering (DLS),⁸ electron microscopy,⁷ and small-angle neutron scattering (SANS).¹⁰ The transition point between these two regions (r_c) depends on the radius of the particle, grafting density of the polymer chains, and the excluded volume parameter of a chain.⁶

Star polymers consist of a number of arms (f) that are bound to a central core and are in many ways analogous to a polymer-grafted nanoparticle, albeit with a very small core, and typically a lower number of grafted chains. For this reason, one might expect that the conformation of a single arm of a star polymer could be slightly stretched from its ideal state. The question of how a starlike polymer architecture affects the conformation of individual branches of the polymer is not a new one, going back at least several decades. The Daoud–Cotton model¹¹ was developed to describe the conformation of star polymers and identifies several regimes along the contour of the arms of the star with differing conformations, which depend on several factors, including f . Generally, portions of the chain that are closer to the core exhibit a larger degree of stretching than those farther away. However, light scattering measurements by Okumoto et al. on high molar mass ($M_w > 100$ kg/mol), six-

Received: January 12, 2017

Revised: February 16, 2017

arm polystyrene dissolved in cyclohexane found no difference in the excluded volume parameter of stars and linear polymers, observing $\nu = 0.5$ at the theta temperature.¹² In benzene, Okumoto et al. observed no difference between four-arm polystyrene stars and linear polymers, measuring $\nu = 0.6$ under good solvent conditions.¹³ SANS measurements by Willner and co-workers¹⁴ studied polybutadiene and polyisoprene with f ranging from 8 to 128 in a good solvent, fitting the scattering data with Benoit's star form factor. Although Benoit's form factor¹⁵ assumes that R_g follows Gaussian statistics by its use of the Debye function, the study was able to determine that the star polymers followed the Daoud–Cotton model by following trends in R_g as a function of f . The authors also observed that both the star form factor and a more detailed form factor derived from renormalization group (RG) techniques¹⁶ failed to describe the scattering results at short distances (high q) when placed on a Kratky plot. Very recently, molecular dynamics simulations by Chremos and Douglas¹⁷ found that for $f = 5$ star polymers adopt a size that scales as $N^{0.43}$ in the melt state. For $f < 5$, the polymers adopt ideal conformations (i.e., $\nu = 0.5$), and the authors predict that as f increases beyond 5, the arms will stretch further leading to an increase in ν , demonstrating how, even for low values of f , small changes in polymer architecture may lead to large changes in polymer melt dynamics—important considerations in polymer processing.

Experimentally, others have observed departures from the expected values for the excluded volume parameter. Kawaguchi et al.¹⁸ studied the radius of gyration of linear poly(*N*-isopropylacrylamide) (PNIPAM) in methanol, synthesized in either benzene or *tert*-butanol by radical polymerization, using light scattering measurements. Interestingly, the authors of this study found that $\nu = 0.55$ for polymers synthesized in *tert*-butanol and $\nu = 0.45$ for polymers synthesized in benzene, concluding that the PNIPAM structure must not be linear. Plummer et al.¹⁹ synthesized four-arm, aromatic-terminated PNIPAM and compared its conformation above and below the lower critical solution temperature (LCST, $T_C \approx 32$ °C) to that of linear PNIPAM using ¹H NMR. Whereas the R_g of linear PNIPAM scaled as $R_g \sim N^{0.5}$ below T_C , the radius of gyration for the star polymer scaled as $R_g \sim N^{0.54}$ at 15 °C, with ν decreasing as T increased, due to the collapse of PNIPAM as T approaches T_C . Lyngsø et al.²⁰ investigated the effect of f on the radius of gyration, LCST, and second virial coefficient (A_2) of PNIPAM star polymers using small-angle X-ray scattering (SAXS) and turbidimetry. T_C was found to decrease as f increased, and compared to linear polymers, the authors also found higher values of A_2 for the star polymers which was attributed to the more particle-like nature of star polymers. The value of A_2 indicated that at 15 °C and below water acts as a good solvent for PNIPAM. In addition, the authors found that Benoit's star form factor was sufficient to fit the scattering data because of the relatively low molar mass of the individual branches, implying that $\nu = 0.5$ for star PNIPAM in water. However, as noted by Willner et al.,¹⁴ this form factor can be used to determine the radius of gyration even under conditions in which the chains are slightly stretched or swollen, meaning the conformation of the star polymers was not uniquely determined. The polymers studied by Lyngsø et al. also exhibited fairly high dispersities ($\mathcal{D} > 1.2$ for $f = 3, 4$, and 6) and had different core chemistries for each value of f , which may make direct comparisons between the polymers challenging. As we demonstrate here, even small changes in the chemical

structure of PNIPAM terminal groups can play a large role in its solution behavior.

This paper describes SANS measurements of star PNIPAM in D₂O for several new purposes. First, we introduce a new form factor for star polymers that explicitly includes excluded volume effects using an excluded volume parameter ν and which is much simpler than the result from RG theory. Second, we perform SANS on solutions of 1 wt % (11 mg/mL) PNIPAM in D₂O for $f = 3, 4$, and 6 and demonstrate that the new form factor fits the data extremely well and allows one to extract both the conformation of a single branch of the polymer and a Flory–Huggins interaction parameter using the random phase approximation (RPA). This new form factor will be an important tool for future scattering studies, especially in relation to applying the RPA to scattering measurements, and can be readily extended to account for looped structures, such as those found in some polymer gels.^{21,22} Multiangle light scattering (MALS) is used to characterize the unique clustering behavior of PNIPAM in aqueous solutions. The star polymers used in this study have nearly identical core chemistries, low dispersities, and a tunable terminal group chemistry—which we show plays a large role in the solution thermodynamics and polymer conformation. Interestingly, PNIPAM stars which are terminated with a short, dodecane chain form compact globules below the LCST, with $\nu \approx 0.38$, despite remaining dispersed in the solution—making such materials potentially interesting for drug delivery applications. Finally, we compare our results to both linear PNIPAM and work from the literature to unify several recent studies of aqueous star PNIPAM.

2. EXPERIMENTAL METHODS

Materials. All materials were purchased from Sigma-Aldrich of the highest quality and used as received unless stated otherwise. *N*-Isopropylacrylamide (NIPAM) (Aldrich, 97%) was recrystallized from toluene/hexane 3:2 and dried by vacuum before use. PNIPAM star polymers were prepared by both atom transfer radical polymerization (ATRP) and reversible addition–fragmentation chain transfer polymerization (RAFT). The 3- and 4-arm star derivatives were synthesized from different chain transfer agents, detailed below. Chain transfer agents 1,1,1-tris[(dodecylthiocarbonothioylthio)-2-methylpropionate]ethane and pentaerythritol tetrakis[2-(dodecylthiocarbonothioylthio)-2-methylpropionate] were purchased from Sigma-Aldrich and used as received.

Synthesis of Pentaerythritol tetrakis(3-(*S*-benzyltrithiocarbonyl)propionate) (PTBTP). PTBTP was synthesized according to Mayadunne et al.²³ Triethylamine (4.04 g, 40 mmol) in 10 mL of CHCl₃ was added dropwise to a stirred solution of pentaerythritol (3-mercaptopropionate) (2.44 g, 5 mmol) and carbon disulfide (3.04 g, 40 mmol) in CHCl₃ (15 mL) at room temperature. The solution was allowed to stir for an additional 1 h. Benzyl bromide (3.76 g, 22 mmol) dissolved in 10 mL of CHCl₃ was added dropwise, and the solution was stirred for a further 2 h. The mixture was poured into a cold solution of 10% aqueous HCl and extracted three times to afford a thick yellow oil. The organic phase was separated and washed three times with saturated sodium chloride solution and dried over Na₂SO₄. The oil was purified by column chromatography using 30% ethyl acetate in petroleum ether as eluent to obtain pentaerythritol tetrakis(3-(*S*-benzyltrithiocarbonyl)propionate) (PTBTP) (4.0 g, 69%). ¹H NMR (600 MHz, CDCl₃) δ (ppm): 2.80 (t, 8H, CH₂), 3.61 (t, 8H, CH₂), 4.14 (s, 8H, CH₂), 4.61 (s, 8H, benzyl CH₂), 7.32 (m, 20H, ArH).

Synthesis of Trimethylolpropanetri-(3-(*S*-benzyltrithiocarbonyl)propanoate). Trimethylolpropane-tris-3-(*S*-benzyl-trithiocarbonyl)propanoate was synthesized according to Edam.²⁴ Triethylamine (1.52 mL, 1.11 g, 10.9 mmol, 3.6 equiv) was added to a solution of trimethylolpropanetri-(3-mercaptopropionate) (1.00 mL, 1.21 g,

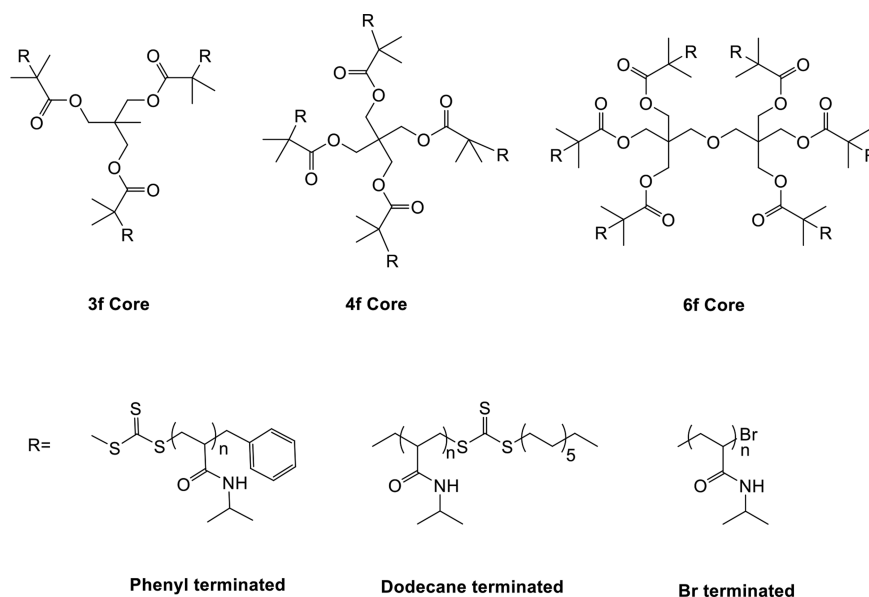


Figure 1. (top) Structures of ATRP star polymer polymer cores for $f = 3, 4,$ and 6 arms. RAFT core structures are similar and contained in the Supporting Information, Figure S7. (bottom) Structures of Br-terminated PNIPAM (ATRP), phenyl-terminated PNIPAM (RAFT), and dodecane-terminated PNIPAM (RAFT).

3.04 mmol) in 50 mL of chloroform. After stirring the reaction mixture for 1 h at room temperature, 5 mL of CS_2 and benzyl bromide (1.30 mL, 1.87 g, 10.9 mmol, 3.6 equiv) were added slowly. The mixture was stirred for 15 h, and the reaction was then quenched by adding 50 mL of 10% hydrochloric acid. The organic phase was separated and washed two times with 50 mL of water and dried over Na_2SO_4 . Solvent and traces of nonreacted starting materials were removed under vacuum to obtain the title compound (2.51 g, 91%). $^1\text{H NMR}$ (600 MHz, CDCl_3) δ (ppm): 0.90 (t, 3 H, CH_3), 1.46 (q, 2 H, CH_2), 2.79 (t, 6 H, CH_2), 3.63 (t, 6 H, CH_2), 4.05 (s, 6 H, CH_2), 4.61 (s, 6 H, CH), 7.32 (m, 15 H, ArH).

Polymerization of Star PNIPAM by RAFT. The 3- and 4-armed PNIPAM terminated with either an phenyl or dodecane group were polymerized by reversible addition–fragmentation chain transfer (RAFT) polymerization. For example, to prepare a 4-armed aromatic PNIPAM with a molar mass of 72 000 g/mol at 80% conversion, a stock solution of NIPAM (10.4 M), azobis(isobutyronitrile) (AIBN) (1.77×10^{-3} M), and chain transfer agent PTBTB (1.33×10^{-2} M) in *N,N*-dimethylformamide (DMF) was prepared. $[\text{NIPAM}]_0 : [\text{CTA}]_0 : [\text{AIBN}]_0 = 780:1:0.13$ Generally, 3 mL of stock solution was transferred to 10 mL Schlenk flasks, connected to a nitrogen manifold, and degassed for 30 min in ice–water bath. Polymerization was conducted at 70 °C in a constant temperature oil bath for 3 h. The flask was opened to the atmosphere and quenched with ice water to terminate the reaction. PNIPAM was dissolved in THF, precipitated with an excess amount of ethyl ether, and then centrifuged for 20 min at 8000 rpm. This precipitation was repeated three times, the solvent was removed, and finally the sample was dried by vacuum to provide polymers with acceptable purity as determined by $^1\text{H NMR}$.

Table 1. PNIPAM Star Characteristics

sample ID	no. of arms (f)	M_n (g/mol)	\bar{D}	terminal group
3f-Br	3	60 100	1.12	Br
4f-Br	4	68 200	1.06	Br
6f-Br	6	92 600	1.08	Br
3f-phenyl	3	45 500	1.19	phenyl
4f-phenyl	4	73 500	1.09	phenyl
3f-alkyl	3	69 700	1.11	dodecane
4f-alkyl	4	92 900	1.07	dodecane

Polymerization of Star PNIPAM by ATRP. Bromine-terminated PNIPAM stars were synthesized by atom-transfer radical polymerization (ATRP).²⁵ A copper chloride catalyst system with tris[2-(dimethylamino)ethyl] (Me_6TREN) as the ligand is used in a monomer:initiator:Cu(I):Cu(II):ligand molar ratio of 158:1:5:0.25:5.25 for each initiation site. 1,1,1-Tris(2-bromo-isobutyryloxymethyl)ethane is the three-arm initiator, pentaerythritol tetrakis(2-bromoisobutyrate) is the four-arm initiator, and dipentaerythritol hexakis(2-bromoisobutyrate) is the six-arm initiator. To synthesize the polymer, a solution of 3 mL of DMF (Fisher Chemical, Certified ACS) with the initiator and monomer was degassed for 20 min in a 25 mL modified Schlenk flask while vigorously stirring. Simultaneously, copper(II) chloride and Me_6TREN were added to 2 mL of DMF in a separate 10 mL modified Schlenk flask and degassed for 20 min, followed by the addition of the copper(I) chloride. After an additional 10 min degassing, the catalyst solution was transferred via syringe to the monomer solution. The solutions were prepared separately, along with a high catalyst ratio, to prevent the nitrogen in NIPAM from coordinating with the copper catalyst, which would potentially reduce its activity by immobilizing it. The reaction was terminated after 3 h by opening the vessel to the ambient atmosphere. The product was then passed through a neutral alumina column in tetrahydrofuran (THF) (Fisher Chemical, HPLC grade) to remove the copper from the system. After the copper removal, the polymer was precipitated in diethyl ether (Fisher Chemical, Certified ACS, BHT stabilized) and centrifuged at 8000 rpm for 20 min.

Size and Molar Mass Characterization. The molar mass and dispersity of the synthesized polymers were determined by size exclusion chromatography (SEC) and multiangle light scattering (MALS) with a differential refractive index detector (Optilab T-rEX, Wyatt Technology Corporation) and an 18-angle static light scattering detector (Dawn Heleos II, Wyatt Technology Corporation) in DMF containing 0.05 mol/L LiBr at a flow rate of 1.0 mL/min. The optical wavelength used by the refractive index and light scattering detectors was 658 nm. The differential index of refraction was measured in DMF with 0.05 mol/L LiBr and determined to be $dn/dc = 0.0638 \pm 0.0016$ mL/g at 25 °C. Data were analyzed using the ASTRA 6.1 software package. Because of the laser wavelength and size of the star polymers ($R_g < 10$ nm), it was not possible to obtain a radius of gyration for the molecules by MALS. The size of PNIPAM clusters in solution were measured by MALS in batch mode from a 20 mL glass scintillation vial. Samples were filtered using a 0.2 μm filter, left undisturbed on the benchtop for at least 24 h to eliminate air bubbles, and thermally

equilibrated until the scattering intensity stabilized before measurements were taken.

Small-Angle Neutron Scattering (SANS). SANS was performed on the NGB 30 m SANS instrument at the National Institute of Standards and Technology (NIST) Center for Neutron Research (NCNR, Gaithersburg, MD) for samples containing 1 wt % of PNIPAM D₂O (11 mg/mL). Scattered neutron intensities were measured as a function of scattering variable q at three sample-to-detector distances of 1, 4, and 13 m. The neutron wavelength was $\lambda = 6 \text{ \AA}$ at the 1 and 4 m detector distances and $\lambda = 8.4 \text{ \AA}$ at the 13 m detector distance. Lenses were used at 13 m to increase the neutron flux on the sample and measure at lower values of q , where the scattering variable $q = (4\pi/\lambda) \sin(\theta/2)$. Two-dimensional scattering patterns were radially averaged and corrected for background and empty sample call scattering using standard methods. The 1D scattering intensities were fit as a function of q using a new form factor which is detailed in the Results section.

3. RESULTS AND DISCUSSION

Small-Angle Neutron Scattering (SANS). The SANS intensities were fit using a form factor for a star branched polymer. The form factor for a single branch of the star polymer with excluded volume is given by

$$P_{\text{sb}}(q, N) = 2 \int_0^1 (1-x) \exp\left[-\frac{q^2 b^2}{6} N^{2\nu} x^{2\nu}\right] dx \quad (1)$$

where ν is the excluded volume parameter, b is the Kuhn length, and q is the scattering variable.²⁶ This integral can be evaluated and expressed in terms of the lower incomplete gamma function, γ , as

$$P_{\text{sb}}(q, N) = \frac{1}{\nu U^{1/2\nu}} \gamma\left(\frac{1}{2\nu}, U\right) - \frac{1}{\nu U^{1/\nu}} \gamma\left(\frac{1}{\nu}, U\right) \quad (2)$$

The variable $U = (qbN^\nu)^2/6$. The form factor for the star polymer with f branches is constructed from the single branch form factor, along with an interbranch “interference” term (depicted in Figures 2a and 2b, respectively):

$$P_{\text{star}}(q, N) = \frac{1}{f^2} [f P_{\text{sb}}(q, N) - f(f-1) P_{\text{ib}}(q, N)] \quad (3)$$

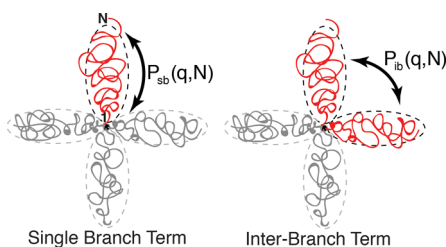


Figure 2. Schematic depiction of the (a) single branch and (b) interbranch form factors from which the form factor of a star polymer with excluded volume is constructed. For the polymer shown, $f = 4$.

where the interbranch form factor reads

$$P_{\text{ib}}(q, N) = 2P_{\text{sb}}(q, 2N) - P_{\text{sb}}(q, N) \quad (4)$$

The interbranch form factor, after some simplification, is derived by analogy to the cross-product term in the binomial formula, i.e., $n_1 n_2 = (n_1 + n_2)^2 - n_1^2 - n_2^2$. $P_{\text{star}}(q, N)$ was combined with the random phase approximation (RPA) to fit the SANS intensities:

$$I(q) = \Delta\rho^2 \left[\frac{1}{N v_p \phi_p P_{\text{star}}(q, N)} + \frac{1}{v_s (1 - \phi_p)} - \frac{2\chi_{\text{ps}}}{\sqrt{v_p v_s}} \right]^{-1} + B \quad (5)$$

where B is the incoherent background, $\Delta\rho$ is the difference in scattering length density between PNIPAM and D₂O ($5.57 \times 10^{-6} \text{ \AA}^{-2}$), v_p is the volume of a NIPAM monomer (161 \AA^3), v_s is the volume of a D₂O molecule (30 \AA^3), ϕ_p is the polymer volume fraction, and χ_{ps} is an interaction parameter between PNIPAM and D₂O. Generally, the molar mass of a polymer can be obtained from the y -intercept of the scattering curve (i.e., the forward scattering intensity at $q = 0 \text{ \AA}^{-1}$), and the size and conformation of the molecule are obtained from the angular (or q) dependence of the scattering intensity. Polymer–solvent interactions, in the form of a nonzero Flory–Huggins parameter or second virial coefficient, lead to slight deviations in the forward scattering intensity as well as nonideal conformations of the chains.

SANS measurements of star polymer systems 3f-Br and 6f-Br are shown in Figure 3 for $T = 5 \text{ }^\circ\text{C}$ (black), $10 \text{ }^\circ\text{C}$ (red), $15 \text{ }^\circ\text{C}$ (blue), and $20 \text{ }^\circ\text{C}$ (green). Solid lines are fits to the model in eq

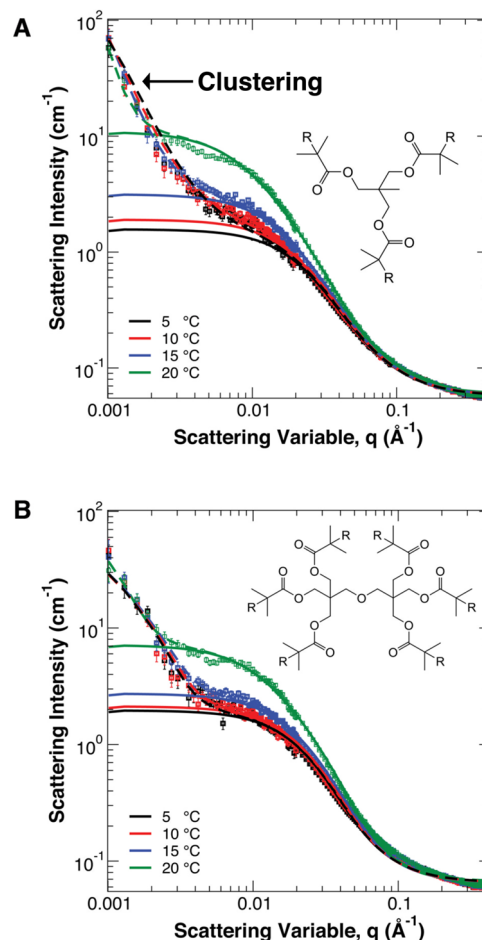


Figure 3. Small-angle neutron scattering (SANS) of Br-terminated PNIPAM stars for (A) $f = 3$ (3f-Br) and (B) $f = 6$ (6f-Br). The solid lines are best fits according to eq 5. The upturn in scattering intensity at low q is attributed to long-range clustering of polymer chains, and the dashed lines are best fits that include an additional term from the Guinier–Porod model²⁷ to describe scattering from large clusters. The error bars correspond to one standard deviation.

5, and dashed lines include an additional Guinier–Porod term²⁷ to describe scattering from polymer clusters at low values of q . The complete set of SANS measurements and fits are contained in the Supporting Information (Figures S8–S13). The general shapes of the SANS curves are consistent with scattering from a polymer and display a power law tail at small values of q representing long-range clustering of the polymer in the solution. This clustering behavior has been studied at length for poly(ethylene oxide) solutions by Hammouda et al.²⁸ using SANS and by light scattering measurements for PNIPAM by Kawaguchi et al.²⁹ but is largely neglected in the literature otherwise. At constant molar mass, the forward scattering intensity, $I(q = 0)$, increases as T increases, which is characteristic of polymer solutions with LCST behavior. At the spinodal temperature, the forward scattering intensity will diverge.

The scattering model in eqs 3 and 5, with only ν and χ_{ps} as free parameters, fits the data well for $T \leq 20$ °C and captures all characteristics of the scattering intensity other than the low- q tail. For both systems in Figure 3, as T increases from 5 to 20 °C, the excluded volume parameter decreases while the interaction parameter increases, indicating the solvent quality is becoming poorer. In all cases, the radius of gyration of the arms of the star polymer fall approximately between 5 and 7 nm, depending on the molar mass and excluded volume parameter for the particular polymer. Bromine-terminated polymers display a strong increase between $T = 15$ °C and $T = 20$ °C, indicating a relatively large increase in the interaction parameter.

The characteristics of the entire star polymer can be determined by fitting the scattering data to a Lorentzian function

$$I(q) = \frac{I_0}{1 + (q\xi)^m} + B \quad (6)$$

where m is the solvation Porod exponent for the entire star polymer, I_0 is a constant scaling factor, ξ is a correlation length, and B is the incoherent background. ξ is a “correlation length” that scales with the radius of gyration of the polymer and can be used to estimate the size of an object in solution. The excluded volume parameter of the entire star polymer is given by $\nu_{\text{star}} = 1/m$. A comparison between ν_{star} and ν (the excluded volume for a single arm) yielded similar values. The Br- and phenyl-terminated star polymers were found to have correlation lengths of approximately 7.5 nm. Assuming the arms adopt Gaussian conformations (i.e., $\nu = 0.5$), the mean-squared radius of a star polymer with f arms and a total degree of polymerization N can be expressed as¹

$$\langle R_g^2 \rangle = \left[\left(\frac{N}{f} \right) \frac{b^2}{6} \right] \left(3 - \frac{2}{f} \right) \quad (7)$$

Using a Kuhn length³⁰ of $b = 6.8$ nm and an average total degree of polymerization of $N = 500$, we estimate that our $f = 4$ star polymers should have an average radius of gyration 7.7 nm, in accord with the results of fitting the data to a Lorentzian model.

The dodecane-terminated polymers had significantly larger correlation lengths. The terminal group of the polymer arms has a large effect on the conformation and clustering/association behavior of star PNIPAM, which is perhaps surprising given the relatively high molar mass of the star polymers compared to the terminal groups. Figure 4 shows

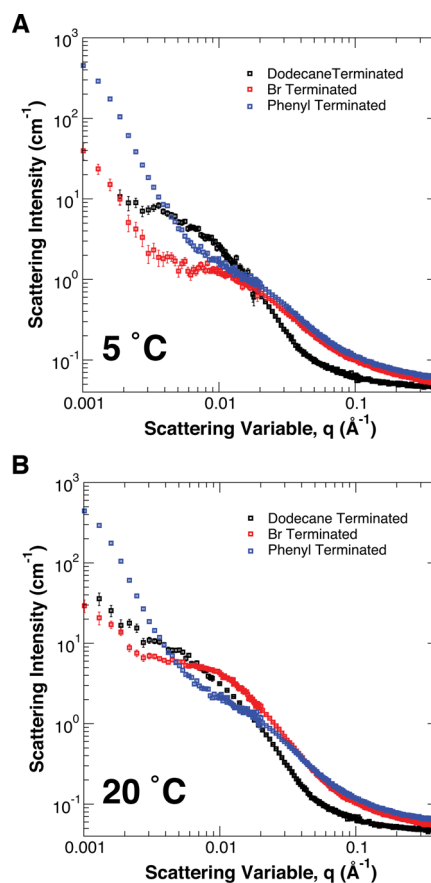


Figure 4. Small-angle neutron scattering (SANS) at (A) 5 °C and (B) 20 °C for dodecane (black), Br (red), and phenyl (blue) terminated star PNIPAM ($f = 4$). Errors bars correspond to one standard deviation.

SANS measurements of 4f-alkyl, 4f-Br, and 4f-phenyl at (A) 5 °C and (B) 20 °C. The difference in conformation between the dodecane-terminated polymer (black) and the two others can be observed from the difference in slope in the scattering curves near $q = 0.02$ Å⁻¹. The greater slope of the dodecane-terminated data indicates a more collapsed structure compared to the Br- and phenyl-terminated polymers. In addition, the slopes of the scattering data for the Br- and phenyl-terminated polymers are similar for $q > 0.02$ Å⁻¹, indicating similar conformations for the Br- and phenyl-terminated polymers. However, the difference in scattering intensity at $q < 0.01$ Å⁻¹ demonstrates differences in the clustering of polymers at large length scales. Specifically, the Br-terminated polymer appears to dissolve better than the phenyl-terminated polymer at 5 °C on the basis of a smaller intensity in the data at low q . However, the reverse is true at 20 °C. This trend is explored in greater detail below. As the temperature increases (Figure 4B), the scattering curves from the dodecane- and phenyl-terminated polymers look qualitatively similar to the 5 °C data, whereas the Br-terminated sample is characterized by a marked increase in scattering intensity in the region near $q = 0.01$ Å⁻¹, indicating that the Br-terminated polymer is interacting less favorably with the solvent than the phenyl-terminated polymer. Unfortunately, it is difficult to further quantify the clustering of the polymers from our SANS measurements, other than noting that the polymers are forming moderate-sized aggregates well below the LCST, as we discuss below.

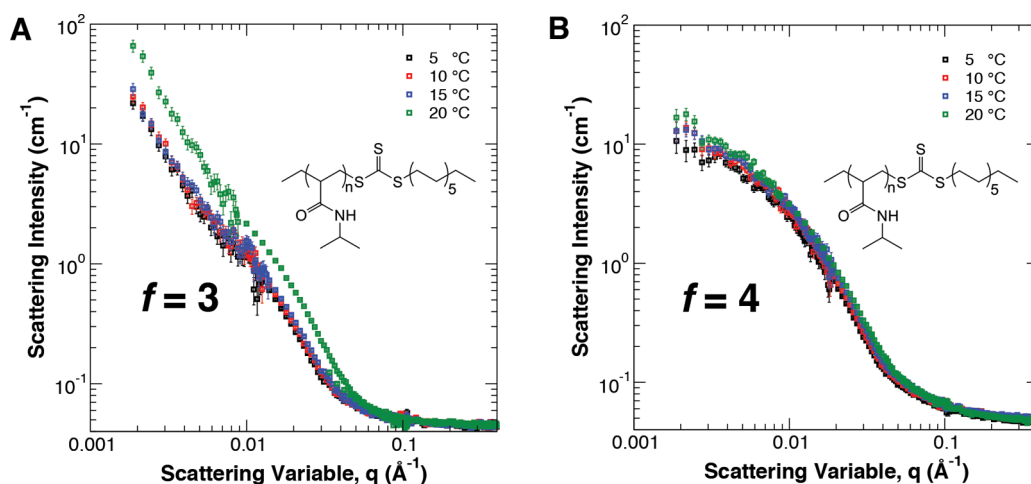


Figure 5. Small-angle neutron scattering (SANS) for the 4f-alkyl sample at 5 °C (black), 10 °C (red), 15 °C (blue), and 20 °C (green). The inset shows the chemical structure of one arm of the dodecane-terminated PNIPAM star.

Dodecane-terminated star PNIPAM exhibits the most complex behavior of the library of polymers. SANS measurements of the (a) 3f-alkyl and (b) 4f-alkyl samples are shown in Figure 5 for $T = 5, 10, 15,$ and 20 °C. For $f = 3$, the scattering intensity is largely described by a power law and does not exhibit a strong temperature dependence below 20 °C. The lack of a temperature dependence in the data suggests that the structures formed in solution remain unchanged. The large tail in the scattering intensity may indicate the formation of a network-like structure throughout the sample due to the amphiphilic-like nature of the 3f-alkyl polymer. Interestingly, for $f = 4$, the large upturn in the scattering curves at low q , observed for the other terminal groups in Figures 3 and 4, is largely absent, showing that the polymers are not forming network-like structures as T increases. This is a particularly interesting result, as it highlights the impact that star polymer functionality and core chemistry have on polymer assembly in solution; polymers with $f = 3$ arms form large, network-like structures whereas those with $f = 4$ arms form discrete, nanoscale aggregates. In both cases, however, LCST behavior is indicated by the small increase in the scattering intensity as T increases. Using the Lorentzian model above eq 6, we determined the correlation length of 3f-alkyl to be $\xi \approx 15$ nm and 4f-alkyl to be $\xi \approx 12$ nm, both of which are larger than the expected size of individual chains ($R_g \approx 7\text{--}8$ nm). This suggests both that the scattering is from aggregates containing multiple polymers and that the aggregates themselves may contain different number of polymers between $f = 3$ and $f = 4$.

Star Polymer Conformation. The conformations of the arms of the star polymers are characterized by the excluded volume parameter ν , with the radius of gyration of each arm scaling as $R_g \sim N^\nu$. Figure 6 plots ν as a function of temperature for all of the star PNIPAM systems. As temperature increases, ν decreases, as expected for a polymer with LCST behavior, and consistent with the well-known coil-to-globule transition for PNIPAM. The terminal group chemistry (Br or phenyl) has only a minor effect on the excluded volume parameter. The conformation of the Br- (solid lines) and phenyl-terminated PNIPAM arms (dashed lines) have only a subtle temperature dependence, with an R_g that roughly scales as $N^{0.51}$ at 5 °C and $N^{0.48}$ at 20 °C, characteristic of near- θ solvent conditions for the polymer. Previous studies have estimated the theta temperature of PNIPAM in H_2O to be 30.6 °C.³¹ No

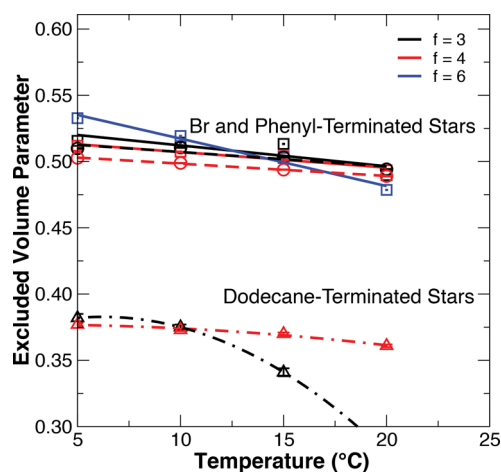


Figure 6. Excluded volume parameter (ν) extracted from least-squares fitting of the SANS data to the RPA model in eq 5. Matched symbols correspond to identical terminal groups, and colors correspond to identical values of f . Lines are guides to the eye. Error bars are smaller than the data points.

substantial difference in the excluded volume parameter is observed between $f = 3$ (black) and $f = 4$ (red), with both sets of polymers exhibiting nearly identical behavior. The excluded volume parameter for Br-terminated arms increases as f increases, with $f = 3$ and $f = 4$ exhibiting very similar values of ν to each other for $T = 5\text{--}20$ °C. The arms of the $f = 6$ polymer are more swollen than the other two $f = 3$ and $f = 4$ polymers, with $R_g \sim N^{0.53}$ at 5 °C, and more collapsed at 25 °C, with $R_g \sim N^{0.47}$. While differences between the conformations of phenyl and Br-terminated stars are small, the general trends with respect to f are in good agreement with the recent predictions by Chremos and Douglas.¹⁷

In contrast to the Br- and phenyl-terminated polymers, the dodecane group has a strong effect on the polymer conformation. The dodecane-terminated star polymers appear to form collapsed globules in solution, where the globules adopt an average size $R_g \sim N^{0.38}$ at 5 and 10 °C. As T increases beyond 10 °C, the similarities between $f = 3$ and $f = 4$ disappear, and the three-armed polymer adopts a more compact conformation than the four-armed polymer. As noted above, the star form factor and RPA could not be

applied to these systems and a Lorentzian model (eq 6) was used to obtain the overall size and conformation of a fractal object in solution. The conformation of the individual arms cannot be obtained from the SANS data in this manner. Nevertheless, information obtained from this model points to scattering from collapsed aggregates that contain several individual star polymers. The precise manner in which the terminal groups associate as the chains pack into globules is currently unknown. Future studies using coarse-grained computer simulations may be able to answer this question. Work from the O'Reilly and Epps groups³² has shown that linear homopolymers terminated with a dodecane chain from the DDMAT chain transfer agent (CTA) tend to form micelles in solution. Thus, the question of how star-branched PNIPAM, with an identical terminal group, assembles in solution to form globules or micelles is an intriguing one to address in the future, considering the unique geometry of star polymers.

Star Polymer Interaction Parameters. Interaction parameters between the polymers and water, χ_{ps} , were obtained from the random phase approximation (RPA), shown in Figure 7. Without a star polymer form factor that can account for

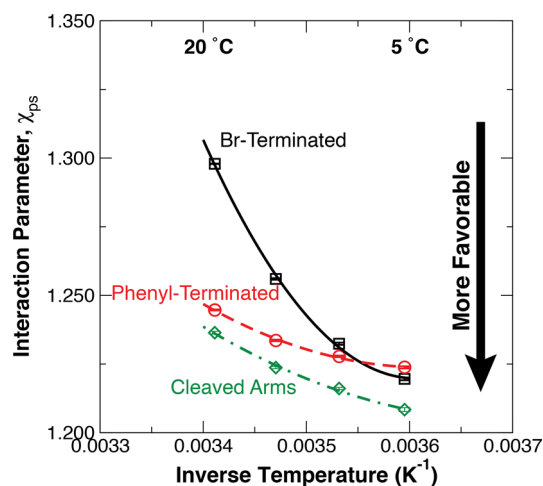


Figure 7. Interaction parameters extracted from SANS measurements using the random phase approximation (RPA). Solid lines correspond to Br-terminated star polymers, and dashed lines correspond to phenyl-terminated polymers. The green points are interaction parameters of linear PNIPAM, produced by cleaving the arms off of the 4f-phenyl sample. The polymer is terminated by a thiol ($-SH$) group on one end and the original phenyl group on the other. Lines are least-squares fits to a quadratic function of inverse temperature. Error bars are smaller than the data points.

excluded volume interactions, extraction of these interaction parameters from SANS measurements would be difficult. Also contained in Figure 7 are the interaction parameters for linear PNIPAM, which was produced by cleaving the arms from the 4f-phenyl sample to produce exact linear analogues of the arms of the star polymers (diamond points). Interaction parameters for the cleaved arms were extracted with the same scattering model, setting $f = 1$. The magnitudes of the interaction parameters are in good agreement with previous measurements of linear PNIPAM in D_2O in which the two ends of the polymer were terminated with carboxylic acid and a short two-carbon alkyl tail, resulting from the use of EDMAT as the CTA in the synthesis.³³

For all terminal groups, the interaction parameters show an increase with temperature indicating less favorable interactions

between PNIPAM and D_2O —characteristic of LCST behavior. We find that bromine-terminated polymers experience less favorable interactions with the solvent than the phenyl-terminated polymers for $T > 5$ °C, with the interaction parameters showing a large increase as T increases. This result is surprising, and we do not have a definitive explanation for this phenomenon, except to note that in the case of phenyl-terminated PNIPAM, polymer arms contain a trithiocarbonate near the core of the polymer as a result of the choice of CTA, whereas the bromine-terminated polymer does not. This could result in a slightly more favorable interaction between the polymer as a whole and the solvent as compared to the case where the trithiocarbonate group is at the chain end. Though surprising, the higher interaction parameter measured for the bromine-terminated polymer is consistent with the behavior of the SANS patterns with respect to temperature, most notably in the large increase in scattering intensity for bromine-terminated PNIPAM versus the phenyl-terminated PNIPAM as temperature increases (cf. Figure 4). In addition, the interaction parameters agree well with our observation that Br-terminated polymers appear to be better dissolved than phenyl-terminated polymers at 5 °C but that the reverse is true at 20 °C. Because the RPA is a mean-field theory, it can only be applied in situations where composition fluctuations are small. The width of the region in which fluctuations are large, and mean-field theory does not apply, is given by the Ginzburg criterion.¹ From a scattering point of view, if mean-field theory is applicable, then the forward scattering intensity should scale as $I(q = 0) \sim (T/T_C - 1)^{-1}$, where T_C is the critical temperature. When fluctuations become an important consideration near the critical temperature, the scaling exponent increases from 1 to 1.26.³⁴ Thus, if the RPA is applicable, then one would expect a linear relationship $1/I(0) \sim 1/T$. Analysis of our measurements confirms this linear relationship (Figure S14), implying that the application of the mean-field RPA theory is valid for our PNIPAM systems and that fluctuations do not play a large role in the scattering behavior at the temperatures for which we have performed measurements, despite the large differences observed between the phenyl- and Br-terminated polymers,

To further investigate the differences between interaction parameters for the phenyl- and Br-terminated PNIPAM, we cleaved the arms from sample 4f-phenyl to produce linear polymers of the exact molecular weight as the star precursor, but which were terminated by a thiol group on one end while retaining the original phenyl terminal group on the other. The rationale in cleaving the arms from the polymer is that by forming a thiol group on one of the chain ends, the interaction between the polymer and solvent should be slightly more favorable due to the additional ability of the polymer to form hydrogen bonds with the solvent. As shown by the diamond points in Figure 7, after cleaving the arms from the core, the magnitudes of the interaction parameters decreased as compared to the star precursor, demonstrating the effect the portion of the chain closer to the core of the star polymer can exert on the interactions between PNIPAM and water. It should be noted, however, that the thiol group in the cleaved arms is chemically distinct from the trithiocarbonate group that is present in the star precursor. Nevertheless, these results clearly illustrate the importance of the PNIPAM synthesis process (i.e., RAFT versus ATRP) and CTA selection on the solution behavior of PNIPAM—including such factors as the LCST, clustering in solution, and formation of larger micellar/globular structures—and highlights the importance of consid-

ering such factors when exploiting the thermoresponsive nature of PNIPAM.

PNIPAM Clustering in Water. The neutron wavelength and configuration of the 30 m SANS instrument prevent measurements of structures larger than about 500 nm, meaning that the large structures PNIPAM forms in solution cannot be fully resolved. In addition, because of the relatively low neutron flux, compared to laboratory-scale X-ray or laser sources, and long counting times at low angles (i.e., low values of q), neutron scattering is not an ideal technique for measuring polymer assembly dynamics or cluster sizes in solution. For this reason, the Br- and phenyl-terminated polymers were measured by MALS to determine an approximate size for clusters and to observe the temperature dependent behavior of the clusters.

MALS measurements of sample 4f-phenyl at 20 °C are shown in Figure 8 along with a fit to the data using a Lorenz–

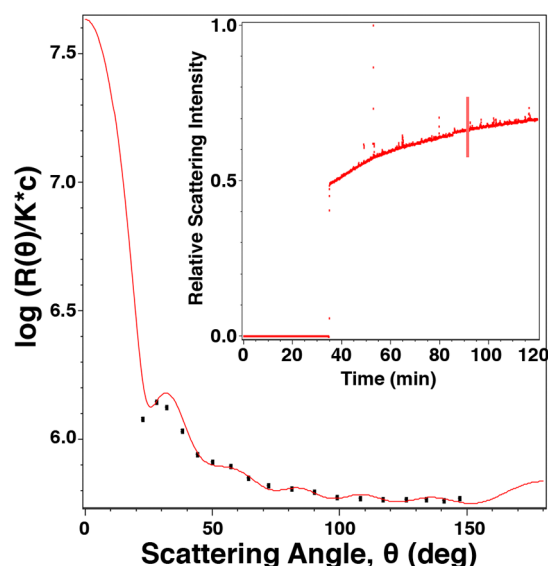


Figure 8. Excess Rayleigh ratio plotted as a function of angle, measured by multiangle light scattering (MALS) for 4f-phenyl at 20 °C. The red line is a fit to Lorenz–Mie scattering of large, spherical objects. The inset shows the light scattering intensity as a function of time. The graduate increase of the intensity signifies the growth of PNIPAM clusters as the vial reaches thermal equilibrium with the instrument. The vertical line is the time point at which the scattering data in the main figure was taken.

Mie scattering model in the ASTRA 6 software package (red line), which results from solving Maxwell's equations to determine the scattering of light from large, spherical objects. The Lorenz–Mie model fits the data reasonably well and yields an average cluster size of 661 ± 5 nm. MALS measurements of other systems (not shown) lack the characteristic oscillations observed in Figure 8 and cannot be fit by the Lorenz–Mie model. We hypothesize the absence of these oscillations is because the clusters are too large to be observed by the instrument, which has an upper size detection limit of approximately $1 \mu\text{m}$. Except for the 4f-phenyl system, all cluster sizes are in excess of $1 \mu\text{m}$.

Though quantitative analysis of MALS data with the Lorenz–Mie model does not find a significant increase in cluster size with temperature, an interesting feature of PNIPAM clusters can be observed in the inset of Figure 8, which shows the relative scattering intensity in the $\theta = 90^\circ$ detector as a function of time as the sample is heated from 20 to 25 °C. An

increase in the scattering intensity in the sample can be attributed to an increase in the size of PNIPAM clusters, since scattering is proportional to the object size. Thus, the scattering intensity reflects the growth of the PNIPAM clusters as temperature increases. Figure S15 shows a similar phenomenon for 3f-Br. Although the present study highlights how minor changes in the chemical structure of PNIPAM polymers alter their solution behavior, future studies might characterize cluster sizes by ultrasmall-angle X-ray scattering (USAXS) or may incorporate fluorescent dyes to observe the clustering of PNIPAM in solution with optical microscopy to connect scattering measurements with real space imaging.

4. SUMMARY

In summary, we have presented a new form factor for star polymers which explicitly accounts for excluded volume and applied it to understanding the behavior of star poly(*N*-isopropylacrylamide) (PNIPAM) in water below the LCST. The new form factor is distinct from the traditional one, introduced by Benoit,¹⁵ which models the arms of the polymer with Debye functions—implying that the arms are Gaussian chains with no excluded volume. While renormalization group (RG) techniques¹⁶ have been used previously to interpret scattering from star polymers with excluded volume, the current approach is more straightforward for routine use and can be combined with the random phase approximation (RPA) to extract interaction parameters between star polymers and a solvent.

Small-angle neutron scattering (SANS) measurements of star-branched PNIPAM found that the number of arms and manner in which the polymer was synthesized both play a role in their behavior in water. Subtle changes to the terminal group changed the interaction parameters and conformation of the arms of the star polymer. In all cases, the value of the excluded parameter indicates that the arms of star-branched PNIPAM adopt slightly swollen conformations as f increases and become more collapsed as temperature increases. Except for dodecane-terminated PNIPAM, which forms globules, all PNIPAM was found to form large clusters in solution at all temperatures. Dodecane-terminated PNIPAM forms large clusters for $f = 3$ but individual dispersed globules for $f = 4$.

While SANS is not able to resolve the size of PNIPAM clusters, multiangle light scattering (MALS) finds that PNIPAM aggregates to form large, micrometer-scale aggregates well below the LCST. The clusters increase in size as temperature increases, but the Lorenz–Mie model is not able to quantitatively capture the increase in size because the cluster size falls outside of the resolution of the MALS instrument. Looking toward the future, additional studies of PNIPAM association and clustering in water and solvent mixtures using fluorescent microscopy and scattering techniques may lead to new types of gels, particles, or thermoresponsive systems for use in a variety of applications, such as payload encapsulation and delivery.

■ ASSOCIATED CONTENT

Supporting Information

The Supporting Information is available free of charge on the ACS Publications website at DOI: 10.1021/acs.macromol.7b00068.

Additional chemical structures, neutron scattering measurements, and multiangle light scattering measurements (PDF)

AUTHOR INFORMATION

Corresponding Author

*(M.J.A.H.) E-mail hore@case.edu.

ORCID

Michael J. A. Hore: [0000-0003-2571-2111](https://orcid.org/0000-0003-2571-2111)

Author Contributions

X.L. and W.R.L. contributed equally.

Notes

The authors declare no competing financial interest.

ACKNOWLEDGMENTS

This work utilized neutron scattering facilities supported in part by the National Science Foundation under Agreement No. DMR-1508249. The identification of commercial products or experimental methods does not imply endorsement by the National Institute of Standards and Technology, nor does it imply that they are the best for the purpose. The authors thank Prof. Emily Pentzer (Case Western Reserve University) for helpful discussions.

REFERENCES

- (1) Rubinstein, M.; Colby, R. H. *Polymer Physics*; OUP: Oxford, 2003.
- (2) Sussman, D. M.; Tung, W. S.; Winey, K. I.; Schweizer, K. S.; Riggelman, R. A. Entanglement Reduction and Anisotropic Chain and Primitive Path Conformations in Polymer Melts under Thin Film and Cylindrical Confinement. *Macromolecules* **2014**, *47* (18), 6462–6472.
- (3) Alexander, S. Adsorption of Chain Molecules with a Polar Head a-Scaling Description. *J. Phys.* **1977**, *38* (8), 983–987.
- (4) Degennes, P. G. Scaling Theory of Polymer Adsorption. *J. Phys.* **1976**, *37* (12), 1445–1452.
- (5) Degennes, P. G.; Pincus, P. Scaling Theory of Polymer Adsorption - Proximal Exponent. *J. Phys., Lett.* **1983**, *44* (7), 241–246.
- (6) Ohno, K.; Morinaga, T.; Takeno, S.; Tsujii, Y.; Fukuda, T. Suspensions of silica particles grafted with concentrated polymer brush: Effects of graft chain length on brush layer thickness and colloidal crystallization. *Macromolecules* **2007**, *40* (25), 9143–9150.
- (7) Choi, J.; Hui, C. M.; Schmitt, M.; Pietrasik, J.; Margel, S.; Matyjaszewski, K.; Bockstaller, M. R. Effect of Polymer-Graft Modification on the Order Formation in Particle Assembly Structures. *Langmuir* **2013**, *29* (21), 6452–6459.
- (8) Dukes, D.; Li, Y.; Lewis, S.; Benicewicz, B.; Schadler, L.; Kumar, S. K. Conformational Transitions of Spherical Polymer Brushes: Synthesis, Characterization, and Theory. *Macromolecules* **2010**, *43* (3), 1564–1570.
- (9) Fernandes, N. J.; Koerner, H.; Giannelis, E. P.; Vaia, R. A. Hairy nanoparticle assemblies as one-component functional polymer nanocomposites: opportunities and challenges. *MRS Commun.* **2013**, *3* (01), 13–29.
- (10) Hore, M. J. A.; Ford, J.; Ohno, K.; Composto, R. J.; Hammouda, B. Direct Measurements of Polymer Brush Conformation Using Small-Angle Neutron Scattering (SANS) from Highly Grafted Iron Oxide Nanoparticles in Homopolymer Melts. *Macromolecules* **2013**, *46* (23), 9341–9348.
- (11) Daoud, M.; Cotton, J. P. Star Shaped Polymers - a Model for the Conformation and Its Concentration-Dependence. *J. Phys.* **1982**, *43* (3), 531–538.
- (12) Okumoto, M.; Tasaka, Y.; Nakamura, Y.; Norisuye, T. Excluded-volume effects in star polymer solutions: Six-arm star polystyrene in cyclohexane near the Theta temperature. *Macromolecules* **1999**, *32* (22), 7430–7436.
- (13) Okumoto, M.; Iwamoto, Y.; Nakamura, Y.; Norisuye, T. Excluded-volume effects in star polymer solutions. Six-arm star polystyrene in benzene. *Polym. J.* **2000**, *32* (5), 422–427.
- (14) Willner, L.; Jucknischke, O.; Richter, D.; Roovers, J.; Zhou, L. L.; Toporowski, P. M.; Fetters, L. J.; Huang, J. S.; Lin, M. Y.; Hadjichristidis, N. Structural Investigation of Star Polymers in Solution by Small-Angle Neutron-Scattering. *Macromolecules* **1994**, *27* (14), 3821–3829.
- (15) Benoit, H. On the Effect of Branching and Polydispersity on the Angular Distribution of the Light Scattered by Gaussian Coils. *J. Polym. Sci.* **1953**, *11* (5), 507–510.
- (16) Alessandrini, J. L.; Carignano, M. A. Static Scattering Function for a Regular Star-Branched Polymer. *Macromolecules* **1992**, *25* (3), 1157–1163.
- (17) Chremos, A.; Douglas, J. F. Communication: When does a branched polymer become a particle? *J. Chem. Phys.* **2015**, *143* (11), 111104.
- (18) Kawaguchi, T.; Kojima, Y.; Osa, M.; Yoshizaki, T. Primary structure of poly(N-isopropylacrylamide) synthesized by radical polymerization. Effects of polymerization solvents. *Polym. J.* **2008**, *40* (6), 528–533.
- (19) Plummer, R.; Hill, D. J. T.; Whittaker, A. K. Solution properties of star and linear poly(N-isopropylacrylamide). *Macromolecules* **2006**, *39* (24), 8379–8388.
- (20) Lyngso, J.; Al-Manasir, N.; Behrens, M. A.; Zhu, K. Z.; Kjoniksen, A. L.; Nystrom, B.; Pedersen, J. S. Small-Angle X-ray Scattering Studies of Thermoresponsive Poly(N-isopropylacrylamide) Star Polymers in Water. *Macromolecules* **2015**, *48* (7), 2235–2243.
- (21) Zhukhovitskiy, A. V.; Zhong, M. Z.; Keeler, E. G.; Michaelis, V. K.; Sun, J. E. P.; Hore, M. J. A.; Pochan, D. J.; Griffin, R. G.; Willard, A. P.; Johnson, J. A. Highly branched and loop-rich gels via formation of metal-organic cages linked by polymers. *Nat. Chem.* **2015**, *8* (1), 33–41.
- (22) Zhukhovitskiy, A. V.; Zhao, J.; Zhong, M. J.; Keeler, E. G.; Alt, E. A.; Teichen, P.; Griffin, R. G.; Hore, M. J. A.; Willard, A. P.; Johnson, J. A. Polymer Structure Dependent Hierarchy in PolyMOC Gels. *Macromolecules* **2016**, *49* (18), 6896–6902.
- (23) Mayadunne, R. T. A.; Jeffery, J.; Moad, G.; Rizzardo, E. Living free radical polymerization with reversible addition-fragmentation chain transfer (RAFT polymerization): Approaches to star polymers. *Macromolecules* **2003**, *36* (5), 1505–1513.
- (24) Edam, R. Comprehensive Characterization of Branched Polymers. Ph.D. Thesis, University of Amsterdam, 2013.
- (25) Teodorescu, M.; Matyjaszewski, K. Controlled polymerization of (meth)acrylamides by atom transfer radical polymerization. *Macromol. Rapid Commun.* **2000**, *21* (4), 190–194.
- (26) Hammouda, B. Form Factors for Branched Polymers with Excluded Volume. *J. Res. Natl. Inst Stan* **2016**, *121*, 139–164.
- (27) Hammouda, B. A new Guinier-Porod model. *J. Appl. Crystallogr.* **2010**, *43*, 716–719.
- (28) Hammouda, B.; Ho, D. L.; Kline, S. Insight into clustering in poly(ethylene oxide) solutions. *Macromolecules* **2004**, *37* (18), 6932–6937.
- (29) Kawaguchi, T.; Kobayashi, K.; Osa, M.; Yoshizaki, T. Is a “Cloud-Point Curve” in Aqueous Poly(N-isopropylacrylamide) Solution Binodal? *J. Phys. Chem. B* **2009**, *113* (16), 5440–5447.
- (30) Zhang, W. K.; Zou, S.; Wang, C.; Zhang, X. Single polymer chain elongation of poly(N-isopropylacrylamide) and poly(acrylamide) by atomic force microscopy. *J. Phys. Chem. B* **2000**, *104* (44), 10258–10264.
- (31) Wu, C.; Wang, X. H. Globule-to-coil transition of a single homopolymer chain in solution. *Phys. Rev. Lett.* **1998**, *80* (18), 4092–4094.
- (32) Patterson, J. P.; Kelley, E. G.; Murphy, R. P.; Moughton, A. O.; Robin, M. P.; Lu, A.; Colombani, O.; Chassenieux, C.; Cheung, D.; Sullivan, M. O.; Epps, T. H.; O'Reilly, R. K. Structural Characterization of Amphiphilic Homopolymer Micelles Using Light Scattering, SANS, and Cryo-TEM. *Macromolecules* **2013**, *46* (15), 6319–6325.

(33) Hore, M. J. A.; Hammouda, B.; Li, Y. Y.; Cheng, H. Co-Nonsolvency of Poly(*n*-isopropylacrylamide) in Deuterated Water/Ethanol Mixtures. *Macromolecules* **2013**, *46* (19), 7894–7901.

(34) Holyst, R.; Vilgis, T. A. Critical-Temperature and Concentration Versus Molecular-Weight in Polymer Blends - Conformations, Fluctuations, and the Ginzburg Criterion. *J. Chem. Phys.* **1993**, *99* (6), 4835–4844.